Journal of Molecular and Cellular Cardiology 46 (2009) 943–951

Contents lists available at ScienceDirect

Journal of Molecular and Cellular Cardiology

journal homepage: www.elsevier.com/locate/yjmcc

Original article

Mitochondrial oxygen tension within the heart

Egbert G. Mik [a,*], Can Ince [b], Otto Eerbeek [b], Andre Heinen [c], Jan Stap [d], Berend Hooibrink [d], Cees A. Schumacher [e], Gianmarco M. Balestra [b], Tanja Johannes [b], Johan F. Beek [f], Ab F. Nieuwenhuis [g], Pepijn van Horssen [h], Jos A. Spaan [h], Coert J. Zuurbier [c]

[a] Department of Anesthesiology, ErasmusMC, University Medical Center Rotterdam, s-Gravendijkwal 230, 3015 CE Rotterdam, The Netherlands
[b] Department of Translational Physiology, Academic Medical Center, University of Amsterdam, The Netherlands
[c] Department of Anesthesiology, Academic Medical Center, University of Amsterdam, The Netherlands
[d] Center for Microscopical Research, Department of Cell Biology and Histology, Academic Medical Center, University of Amsterdam, The Netherlands
[e] Department of Experimental Cardiology, Academic Medical Center, University of Amsterdam, The Netherlands
[f] Laser Center, Academic Medical Center, University of Amsterdam, The Netherlands
[g] Laser Physics and Nonlinear Optics Group, MESA+ Institute for Nanotechnology, University of Twente, Enschede, The Netherlands
[h] Department of Biomedical Engineering and Physics, Academic Medical Center, University of Amsterdam, The Netherlands

ARTICLE INFO

Article history:
Received 3 December 2008
Received in revised form 4 February 2009
Accepted 4 February 2009
Available online 13 February 2009

Keywords:
Mitochondria
Delayed fluorescence
In vivo
Langendorff
Mitochondrial PO_2
Protoporphyrin IX

ABSTRACT

By using a newly developed optical technique which enables non-invasive measurement of mitochondrial oxygenation (mitoPO_2) in the intact heart, we addressed three long-standing oxygenation questions in cardiac physiology: 1) what is mitoPO_2 within the in vivo heart?, 2) is mitoPO_2 heterogeneously distributed?, and 3) how does mitoPO_2 of the isolated Langendorff-perfused heart compare with that in the in vivo working heart? Following calibration and validation studies of the optical technique in isolated cardiomyocytes, mitochondria and intact hearts, we show that in the in vivo condition mean mitoPO_2 was 35 ± 5 mm Hg. The mitoPO_2 was highly heterogeneous, with the largest fraction (26%) of mitochondria having a mitoPO_2 between 10 and 20 mm Hg, and 10% between 0 and 10 mm Hg. Hypoxic ventilation (10% oxygen) increased the fraction of mitochondria in the 0–10 mm Hg range to 45%, whereas hyperoxic ventilation (100% oxygen) had no major effect on mitoPO_2. For Langendorff-perfused rat hearts, mean mitoPO_2 was 29 ± 5 mm Hg with the largest fraction of mitochondria (30%) having a mitoPO_2 between 0 and 10 mm Hg. Only in the maximally vasodilated condition, did the isolated heart compare with the in vivo heart (11% of mitochondria between 0 and 10 mm Hg). These data indicate 1) that the mean oxygen tension at the level of the mitochondria within the heart in vivo is higher than generally considered, 2) that mitoPO_2 is considerably heterogeneous, and 3) that mitoPO_2 of the classic buffer-perfused Langendorff heart is shifted to lower values as compared to the in vivo heart.

1. Introduction

Mitochondria figure prominently in cardiac physiology by powering virtually all forms of mechanical and chemical work of the heart. These organelles can also play a decisive role in cell death and survival signaling. Oxygen is the underlying, ultimate molecule used by the mitochondria, thus giving it the essential role in dictating life or death. The partial pressure of oxygen within the mitochondria (mitoPO_2) is hypothesized to have a regulatory function in important physiological processes such as energy production, radical production, oxygen sensing, and gene expression [1–5]. Surprisingly, no direct quantitative data concerning the in vivo mitoPO_2 within the intact heart are available in the literature.

MitoPO_2 can be estimated from PO_2 values reported for other compartments such as the cytosolic, tissue or vascular compartments. Interestingly, most studies report rather low PO_2 values ranging from 10–17 mm Hg for vascular and interstitial compartments [6–8] to 3–7 mm Hg for the cytosolic compartment [9–11]. Such low values suggest that the oxygen tension at the mitochondria, being at the lowest end of the diffusion pathway which oxygen must travel, is below 5 mm Hg, making it likely that oxygen regulates energy production [1,3,5]. These values deviate largely from other studies, however, which report cardiac microvascular PO_2 values of 50–70 mm Hg [12] or interstitial values of 45 mm Hg [13]. Using these latter, higher values, mitoPO_2 is estimated to be between 20 and 40 mm Hg. To resolve these conflicting estimated data on such an important (patho)physiological parameter of the heart, our first goal of the present study was to provide a direct determination of mitoPO_2 within the intact heart. To this end, we employed a novel optical technique

* Corresponding author. Tel.: +31 6 47890339; fax: +31 10 7033722.
E-mail address: e.mik@erasmusmc.nl (E.G. Mik).

0022-2828/$ – see front matter © 2009 Elsevier Inc. All rights reserved.
doi:10.1016/j.yjmcc.2009.02.002

using oxygen-dependent quenching of the delayed fluorescence lifetime from mitochondrial protoporphyrin IX (PpIX) [14,15].

In addition, although spatial heterogeneity of blood flow, oxygen delivery and oxygen metabolism within the heart is well accepted [12,16,17], it is not known whether such heterogeneity extends to the oxygenation status of mitochondria. Aside from heterogeneity dictated by blood flow distribution, heterogeneity may also exist due to the distribution of mitochondria within the cardiomyocyte, i.e., subsarcolemmal and interfibrillar mitochondria [18]. When mitoPO_2 heterogeneity is present, the determination of a single averaged mitoPO_2 for the whole heart is misleading in that a significant, albeit small, part of all mitochondria within the heart may still be oxygen limited. Thus, a second goal of the present study entailed the determination of mitoPO_2 heterogeneity using a lifetime-deconvolution algorithm developed by Golub et al. [19].

Finally, we wanted to compare the mitochondrial oxygenation status in the isolated, Langendorff-perfused heart with that in the in vivo working heart. Investigations with isolated hearts are numerous, and the results obtained have been used to further our understanding of heart physiology, so that the validity of this model is of utmost importance [20]. We are not aware of other studies that have directly compared the mitochondrial oxygenation status of the isolated heart with that of the in vivo heart, and as such, this direct comparison will aid in answering questions concerning the validity of the isolated heart model.

In the present study we used a novel optical technique [14,15], which allowed for the first time quantitative and non-invasive measurements of mitoPO_2 in the intact heart. Following validation of our technique for determination of mitoPO_2 within the heart, our observations demonstrated rather high mean mitoPO_2 values of 35 mm Hg in the in vivo heart. However, cardiac mitoPO_2 was considerably heterogeneous, such that 10% of mitochondria in the in vivo condition and 30% of mitochondria in the isolated Langendorff-perfused condition still had a mitoPO_2 between 0 and 10 mm Hg, despite the relatively high mean mitoPO_2. Only in the maximal vasodilated condition did the mitochondrial oxygenation status of the isolated heart mimic that of the in vivo heart.

2. Materials and methods

2.1. Animals

Male Wistar rats (Charles River, Wilmington, MA), 38 animals in total with body weight of 351 ± 7 g, were anesthetized with 60 mg/kg pentobarbital and received 5-aminolevulinic acid (ALA; 200 mg/kg dissolved in PBS (100 mg/ml)) through the tail vein, 2–5 h before experimentation or saline (controls). The protocol was approved by the Animal Research Committee of the Academic Medical Center at the University of Amsterdam. Animal care and handling were performed in accordance with the guidelines for Institutional and Animal Care and Use Committees (IACUC).

2.2. Isolated cardiomyocytes

Hearts ($n = 4$) were excised from pentobarbital-anesthetized animals and cardiomyocytes isolated according to previous reports [21]. Cardiomyocytes were kept in albumin-free, low Ca^{2+}-containing Krebs–Henseleit solution until measurements.

2.3. Fluorescence microscopy

Fluorescence microscopy was performed using a Leica fluorescence microscope (DM RA HC) with a cooled CCD camera (KX1400, Apogee Instruments, Roseville, CA) and CY3 band pass filter set. Detection of protoporphyrin IX (PpIX) and MitoTracker Green was similar to that previously reported [15]. Cardiomyocytes were incubated with MitoTracker Green (27 nM for 30 min) and contraction inhibited with butanedione monoxime (BDM; 20 mM). PpIX bleaches rapidly, and we used this property to separate PpIX fluorescence from other sources of autofluorescence [15]. Two successive illuminations of 30 s were performed while integrating the fluorescence images on the cooled CCD. The second image was subtracted from the first image using Image-Pro Plus software (Media Cybernetics, Bethesda, MD). The resulting "bleached image" represented the true PpIX signal. MitoTracker Green images were acquired with a 2 s integration time.

2.4. Flow cytometry

Cardiomyocytes were isolated from hearts of either ALA-treated or saline-treated animals (control). The PpIX fluorescence was studied in control and ALA cells with a LSRII flow cytometer (LSRII, BDbioscience San Jose, CA). To study PpIX fluorescence, the viable cardiomyocytes were gated from a FSC (forward scatter) and SSC (side scatter) dotplot, and PpIX was excited by the blue laser (488 nm) and fluorescence was detected at 695 nm.

2.5. Imaging cryomicrotome

Hearts from ALA-treated and saline-treated animals were rinsed with saline solution and submerged together in a solution of carboxymethylcellulose sodium solvent (Brunschwig Chemie, Amsterdam) and Indian ink (Royal Talens, Apeldoorn) and frozen at −20 °C in an imaging cryomicrotome [22]. The frozen hearts were serially sectioned from base to apex into 17 μm slices. After each cut, images were taken from the cutting plane of the remaining bulk using a 4000×4000 pixel camera (ALTA U16, Apogee Instruments, Roseville, CA) equipped with a 70–180 mm Nikon lens, with excitation set at 510/20 nm and fluorescence detected at 635/30 nm.

2.6. Calibration of the PpIX delayed fluorescence lifetime with partial oxygen tension in cardiomyocytes

A cardiomyocyte suspension of 2 ml was placed in a custom-made cell oxygenator [15]. An adjustable gas-mixture of O_2, N_2 and 5% CO_2 was blown over the cell suspension with $\%O_2$ set at 0, 1, 2, 3, 4 or 5%. Oxygen consumption was inhibited using KCN (10 mM), rotenone (4 μM) and diphenyleneiodonium (DPI; 40 μM).

2.7. Evaluation of the calibration of the PpIX delayed fluorescence lifetime in isolated hearts

To test the feasibility of the calibration of PpIX delayed fluorescence lifetime obtained in isolated cardiomyocytes for use in the intact heart, we performed PpIX lifetime measurements in Langendorff-perfused hearts ($n = 3$) perfused with 2 mM potassium cyanide, 25 mM KCl and 0 mM $CaCl_2$ to prevent contraction and oxygen consumption of the heart. For each heart, the perfusate was equilibrated with two different $\%O_2$ levels between 0 and 7%, balanced with N_2 and 5% CO_2. Oxygen tension was measured in the inflow just above the heart using a needle-type fiber-optic microsensor (World Precision Instruments, Sarasota, FL).

2.8. Isolated mitochondria and effects of ALA administration

Mitochondria were isolated from hearts of animals treated with ALA (200 mg/kg) dissolved in PBS ($n = 3$) or with PBS only ($n = 3$), 3–5 h before isolation. Procedures of isolation were as reported previously [23]. In short, hearts were placed in isolation buffer (200 mM mannitol, 50 mM sucrose, 5 mM KH_2PO_4, 5 mM MOPS, 1 mM EGTA, and 0.1% BSA) and minced into small pieces; then 5 U/ml protease was added, and the mixture was homogenized. The homogenate was centrifuged at 3220 *g* for 10 min, and the pellet was

resuspended in isolation buffer and centrifuged at 800 *g* for 10 min. The remaining supernatant was centrifuged at 3220 *g* for 10 min. The final pellet was resuspended in isolation buffer and kept on ice, and the protein content was determined by the Bradford method.

All procedures were performed at 4 °C. Mitochondrial oxygen consumption was measured polarographically at 37 °C in a respirometer using mitochondria (0.3 mg protein/ml) resuspended in respiration buffer [23]. Respiration was initiated with 10 mM succinate + 10 μM rotenone (state 2 respiration), followed by the addition of 200 μM ADP (state 3 respiration). The respiratory control index (RCI) was calculated as the state-3 to state-4 ratio.

2.9. In vivo hearts

Animals ($n = 5$) were anesthetized with s-ketamine (150 mg/kg) and diazepam (1.5 mg/kg), and maintenance anesthesia was provided through i.v. administration of α-chloralose (30 mg/kg/h). Mechanical ventilation (70 breaths per min, 0.4 inspiration phase, 5 mm Hg PEEP) was started following intubation, and a left thoracotomy was performed to expose the heart [24]. Mean arterial pressure and heart rate were monitored through a fluid-filled catheter positioned in the cannulated carotid artery. Body temperature was maintained at 37 °C. Inspiration oxygen fraction was initially set at 40% and subsequently switched to 100% and finally 10% O_2. The 40% FiO_2 step was deliberately chosen instead of 20% FiO_2 to ensure compensation for ventilation-perfusion defects due to mechanical ventilation [25] resulting in arterial PO_2 values in the physiological range reported for spontaneously air-breathing animals (~120 mm Hg).

2.10. Microvascular PO_2 of the in vivo hearts

To compare the mitoPO_2 with other indices of cardiac oxygenation, cardiac microvascular PO_2 (μPO_2) of the in vivo heart was determined in separate animals ($n = 4$) by the method of oxygen-dependent quenching of the phosphorescence lifetime of intravenously injected Pd-porphyrin (Pd-*meso*-tetra(4-carboxyphenyl)porphine, Frontier Scientific Inc, Logan, UT). To this end Pd-porphyrin was bound to albumin according to Sinaasappel et al. [26] and intravenously injected (12 mg/kg). Phosphorescence signals were obtained from the in vivo rat heart using a fiber based phosphorimeter [27]. These measurements were performed in a similar in vivo heart model as

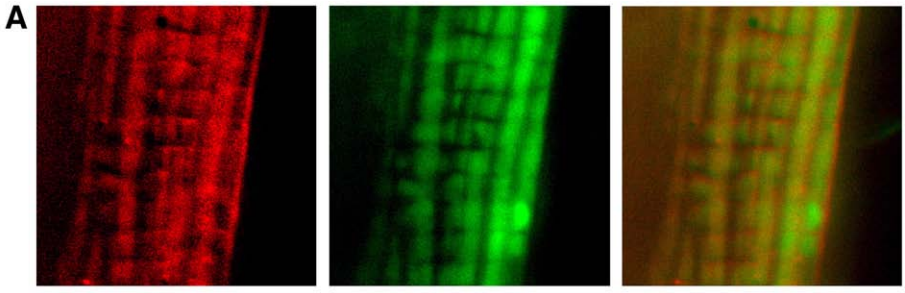

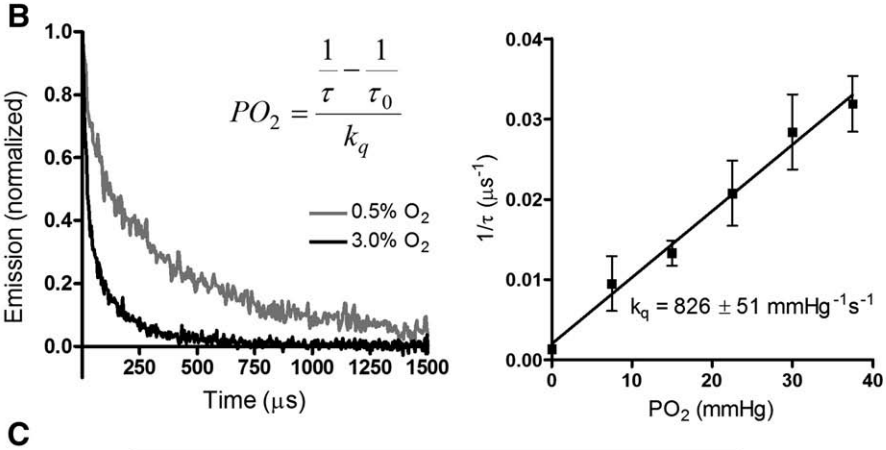

C

	Control	ALA	p-value
State 3	275 ± 8*	272 ± 2*	0.57
State 4	105 ± 5*	103 ± 6*	0.63
RCI	2.61 ± 0.15	2.66 ± 0.13	0.72
ADP/O	1.74 ± 0.11	1.75 ± 0.07	0.89

* Respiratory rate in nmol O_2 · min^{-1} · mg $protein^{-1}$

Fig. 1. PpIX in cardiomyocytes and mitochondria. (A) Fluorescence microscopy showing (from left to right) PpIX fluorescence, MitoTracker Green fluorescence and colocalization of PpIX and Mitotracker Green fluorescence in isolated cardiomyocyte. (B) In vitro calibration experiments showing two examples of delayed fluorescence traces recorded at two different oxygen concentrations and the reciprocal delayed fluorescence lifetime ($1/\tau$) versus PO_2 in suspensions of isolated cardiomyocytes. Inserted is the Stern–Volmer equation in which k_q is the quenching constant and τ_0 is the lifetime at zero oxygen. Lifetimes were retrieved from the data by a mono-exponential non-linear Marquart–Levenberg fitting procedure. Shown are the mean and SD. (C) Function of mitochondria isolated from hearts of control or ALA-treated animal showing state 3 and 4 respiration, respiratory control index (RCI) and the P/O ratio.

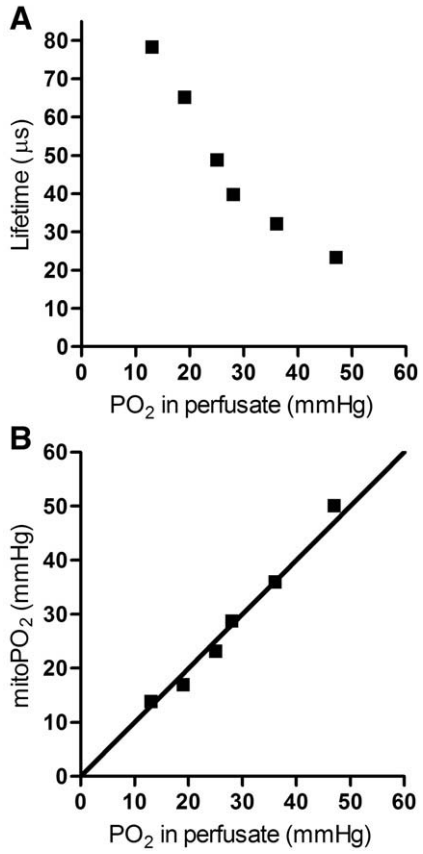

Fig. 2. Evaluation of the calibration constants in isolated rat heart. (A) Measured delayed fluorescence lifetime versus the PO_2 in the perfusate after cessation of mitochondrial oxygen consumption by addition of cyanide. Lifetimes were retrieved from the data by a mono-exponential non-linear Marquart–Levenberg fitting procedure. (B) MitoPO_2 versus the PO_2 in the perfusate. MitoPO_2 was calculated from the delayed fluorescence lifetimes in panel A using the quenching constants obtained in suspensions of cardiomyocytes. The solid line is the line of equality.

used for the PpIX determinations, at FiO_2 of 40%, 100% and 10%, respectively (see description above).

2.11. Isolated Langendorff-perfused hearts

Hearts were isolated from pentobarbital-anesthetized animals and perfused at constant flow at 80 mm Hg according to previous reports [28]. Hearts ($n=6$) were paced at 300 beats/min, and a balloon was inserted in the left ventricle to record left ventricular pressure. The perfusate contained glucose (10 mM/l), pyruvate (0.1 mM/l), lactate (1 mM/l), and glutamine (0.5 mM/l) as substrates. Venous oxygen tension was measured in the pulmonary artery using a needle-type fiber-optic microsensor (World Precision Instruments, Sarasota, FL). Perfusate was equilibrated with either 95%/0%/5%, 70%/25%/5% or 45%/50%/5% of $O_2/N_2/CO_2$, respectively, using separate calibrated gas bottles. In a separate series ($n=6$), the effect of maximal vasodilatation (100 μM adenosine and 1 μM nitroprusside) on the oxygenation status was studied.

2.12. Delayed fluorescence setup

The setup was essentially the same as that described previously [14]. In short, the excitation source was a tunable laser providing pulses of 2–4 ns (510 nm, 0.2 mJ/pulse). The detector was a red-sensitive photomultiplier tube combined with a monochromator set at 640 nm. Signal processing was done with a home-built integrator with an integration time of 3.5 μs and a reset time of 0.5 μs. A PC-based data-acquisition system sampled the signal at 250 kHz and averaged 64 laser pulses (repetition rate 20 Hz) prior to analysis. Controller and data-acquisition software was written in LabView (Version 7.1, National Instruments, Austin, TX).

2.13. Recovery of mitoPO_2 histograms

In case of a non-homogenous mitoPO_2, the delayed fluorescence signal can be described generally by an integral over an exponential kernel:

$$y(t) = \int_0^t \exp(-\lambda t) f(\lambda)$$

where $f(\lambda)$ denotes the spectrum of reciprocal lifetimes that should be determined from the finite data set $y(t)$. According to Golub et al. [19], a detailed recovery of the underlying oxygen distribution can be obtained by assuming that the delayed fluorescence signal can be described by a sum of rectangular distributions with adequately small chosen width (2δ), resulting in the following fit equation:

$$Y^*(t) = Y(t)\left[\exp(k_0 t) k_q \delta t / \sinh(k_q \delta t)\right] = \sum w_i \exp(-k_q Q_i t)$$

where $Y(t)$ is the normalized phosphorescence data, k_0 is the first-order rate constant for delayed fluorescence decay in the absence of oxygen, k_q is the quenching constant, and w_i is the weight factor for the according bin with central PO_2 Q_i and width 2δ ($w_i \geq 0$ and $\sum w_i = 1$). Recently, this approach was successfully used by our group for the recovery of microvascular PO_2 histograms from phosphorescence lifetime measurements [29] and mitoPO_2 histograms from delayed fluorescence lifetime measurements in rat liver in vivo [14]. Recovery of oxygen histograms from the photometric signal was performed with the GraphPad Prism package (Version 4, GraphPad Software Inc, San Diego, CA). Mean mitoPO_2 values were calculated from the retrieved mitoPO_2 histograms.

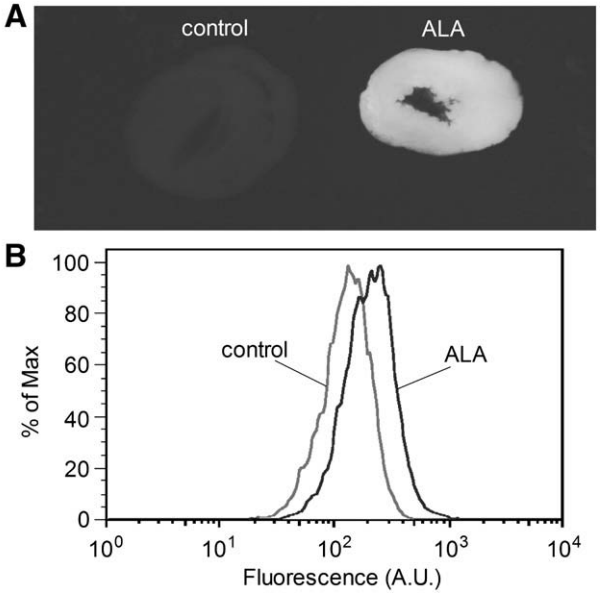

Fig. 3. Distribution of ALA enhanced PpIX in the myocardium. (A) Typical example of an image obtained in the cryomicrotome showing PpIX fluorescence in hearts from a control (saline treated) and an ALA treated animal. Excitation at 510 nm, emission at 630 nm. (B) Flow cytometry in cardiomyocytes isolated from a control and ALA treated animal. Excitation at 488 nm, emission at 695 nm. The histograms are normalized to the maximal counted number of cells having equal fluorescence intensity (% of Max), i.e. the peaks of the individual histograms.

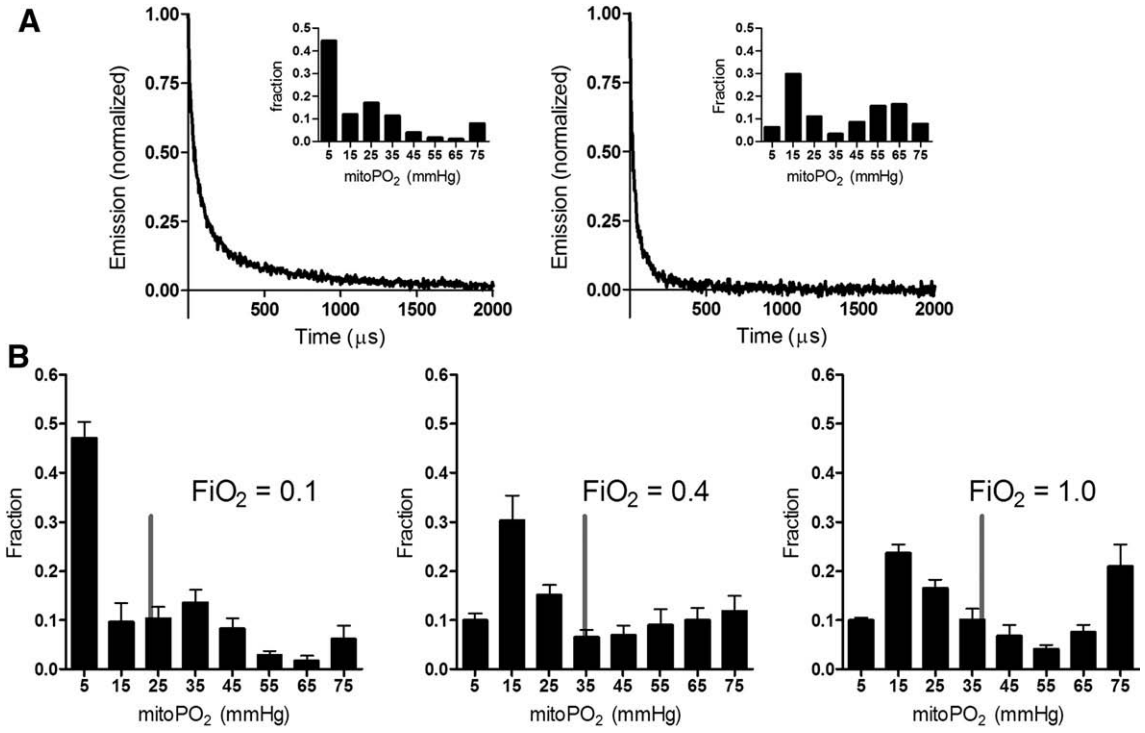

Fig. 4. MitoPO$_2$ in the in vivo heart. (A) Delayed fluorescence traces from the heart of an animal ventilated with 10% oxygen (left panel) and 40% oxygen (right panel). (B) Distributions of mitoPO$_2$ at different FiO$_2$ ($n = 5$). The grey lines denote the mean mitoPO$_2$.

2.14. Chemicals

Mitotracker Green was obtained from Invitrogen (Carlsbad, CA). Pentobarbital was obtained from Ceva (Sante Animale B.V., Maassluis, The Netherlands), Diazepam from Centrafarm (Etten-Leur, The Netherlands), S-ketamine from Pfizer B.V. (Capelle a/d IJssel, The Netherlands) and PBS was obtained from Baxter. ALA, α-chloralose, KCN, rotenone, DPI, BDM, KH_2PO_4, MOPS, EGTA, BSA, protease, mannitol, succinate, pyruvate, sucrose, lactate, glucose, glutamine, adenosine, nitroprusside and the compounds for the Krebs–Henseleit buffer were all obtained from Sigma (St. Louis, MO).

2.15. Presentation of data

The data are presented as mean ± SEM, unless stated otherwise.

3. Results

3.1. Subcellular location of PpIX

Four hours after ALA administration, we observed a similar nonhomogeneous cellular distribution of PpIX fluorescence and MitoTracker Green signals in isolated cardiomyocytes (Fig. 1A). The very high colocalization of both images indicates the mitochondrial localization of the PpIX signal.

3.2. Calibration of the mitochondrial signal

Oxygen-dependent delayed fluorescence traces were clearly detectable from cardiomyocyte suspensions subjected to various oxygen levels. The calibration curve of reciprocal lifetime versus partial oxygen pressure for cardiomyocytes demonstrated a quenching constant (k_q) that was similar to the k_q obtained in hepatocytes [14], indicating the general applicability of the calibration constant across organs (Fig. 1B). Lifetime under zero oxygen conditions (τ_0) was 0.8 ms.

3.3. ALA treatment does not affect mitochondrial oxygen consumption (Fig. 1C)

In order to examine whether ALA-induced mitochondrial accumulation of PpIX affected mitochondrial oxygen consumption, mitochondria were isolated from ALA-treated and vehicle-treated animals. PpIX accumulation had no effect on respiration, coupling ratio or oxidative phosphorylation of the mitochondria, demonstrating that ALA-treatment did not disturb oxygen consumption.

3.4. Validation of the calibration constants in isolated rat heart

To test the validity of the calibration constants obtained from the isolated cardiomyocytes in intact heart we measured the delayed fluorescence lifetime in isolated Langendorff-perfused hearts from ALA treated animals. Oxygen consumption was blocked by addition of cyanide and measurements were performed at varying oxygen tensions in the perfusate. Blockage of oxygen consumption abolishes the oxygen gradients in the tissue and mitoPO$_2$ should equal the PO$_2$ in the perfusate. Mono-exponential fitting of the delayed fluorescence signals showed clearly oxygen-dependent delayed fluorescence lifetimes (Fig. 2A). Conversion of the lifetimes into mitoPO$_2$ values using the calibration constants $k_q = 826$ mm Hg^{-1} s^{-1} and $\tau_0 = 0.8$ ms obtained from cardiomyocyte suspensions resulted in

Table 1
Hemodynamics and blood gas values of rats in vivo ($n = 5$)

F_iO_2 %	MAP mm Hg	Heart rate Beats/min	PaO_2 mm Hg	$PaCO_2$ mm Hg	tHb mmol/l
40	99 ± 5	351 ± 21	115 ± 5	41 ± 3	6.9 ± 0.5
100	103 ± 6	336 ± 20	331 ± 20	43 ± 6	6.2 ± 0.7
10	50 ± 5	305 ± 15	39 ± 3	40 ± 2	6.2 ± 0.7

F_iO_2 = inspiration oxygen %; MAP = mean arterial pressure; PaO_2 = partial arterial oxygen tension; $PaCO_2$ = partial arterial carbon dioxide tension; tHb = total hemoglobin. Values are given as mean ± SEM.

excellent agreement between mitoPO$_2$ and the PO$_2$ in the perfusate (Fig. 2B).

3.5. Distribution of ALA enhanced PpIX

Our analysis method assumes that PpIX is homogenously distributed in the measurement volume. For proper interpretation of our data it is essential to know to what extend this assumption holds in practice. Images from the cryomicrotome clearly showed increased, diffuse and near homogeneous red fluorescence throughout the entire myocardium after ALA administration (Fig. 3A). Some local differences in fluorescence intensity were visible, but this comprised relatively large areas also visible in the control heart. Therefore these differences might be due to fixation and cutting artifacts instead of true heterogeneities in the PpIX distribution. This was indeed confirmed by the flow cytometry experiments, which showed a uniform emergence of red fluorescence after administration of ALA (Fig. 3B).

3.6. MitoPO$_2$ in the in vivo heart

FiO$_2$-dependent delayed fluorescence signals were obtained from in vivo rat heart (Fig. 4A). At 40% FiO$_2$, the largest fraction (26%) of mitochondria was found in the range of 10–20 mm Hg, with a mean mitoPO$_2$ of 35 ± 5 mm Hg (Fig. 4B). Increasing Fi0$_2$ to 100% had no major effect on the mitoPO$_2$ distribution; however, reducing FiO$_2$ to 10% resulted in large changes: 46% of the mitochondria were in the lowest oxygen range of 0–10 mm Hg (Fig. 4B). The imposed FiO$_2$ changes were accompanied by alterations in arterial oxygen tension and blood pressure, without changes in arterial CO$_2$ tension (Table 1).

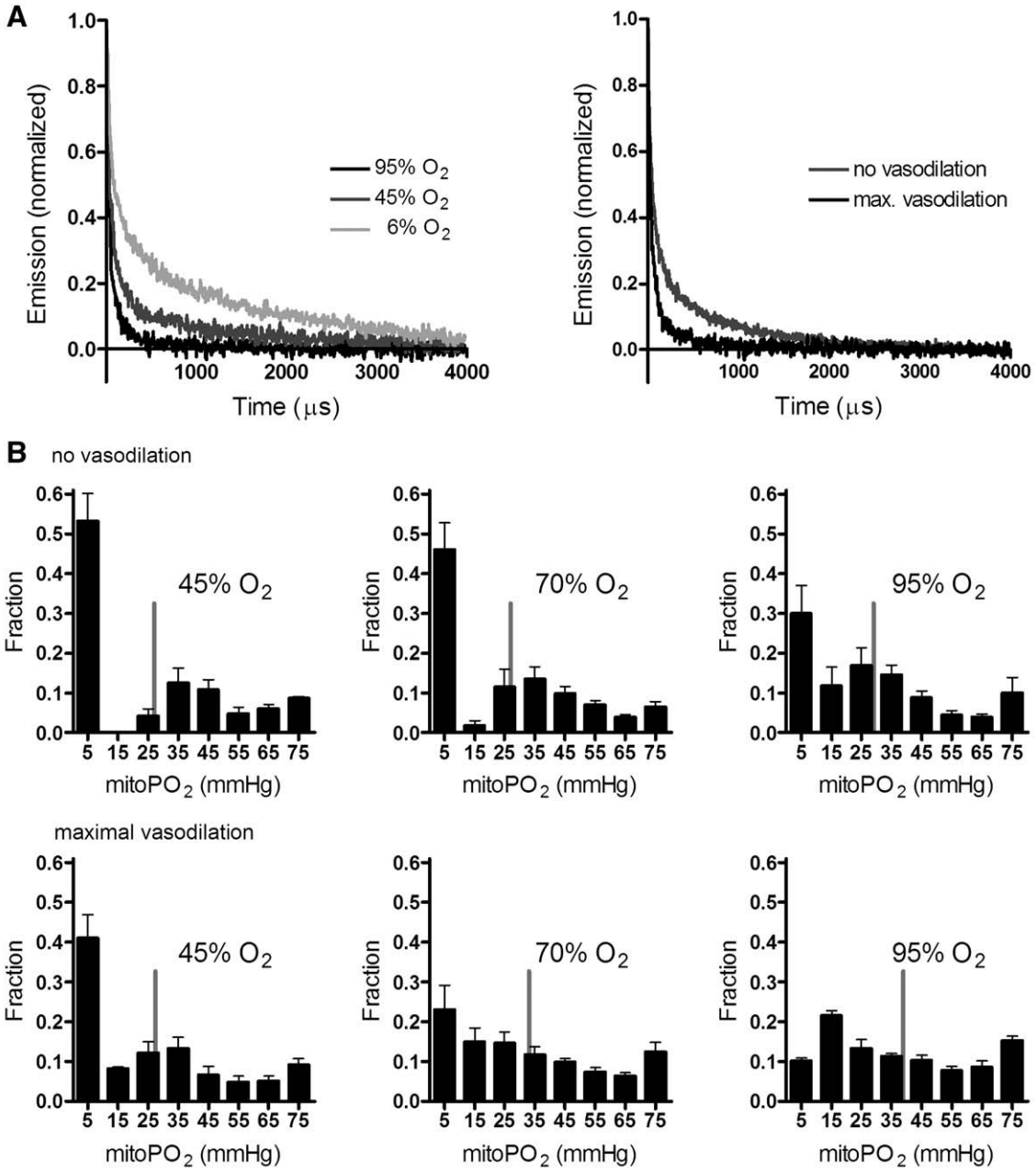

Fig. 5. MitoPO$_2$ in the isolated Langendorff-perfused heart. (A) Examples of delayed fluorescence traces for 95%, 45%, and 6% oxygen saturated perfusate in a vasodilated heart (left panel) and delayed fluorescence traces of a normal and maximally vasodilated heart (right panel). (B) Distributions of mitoPO$_2$ at different %O$_2$ in perfusate for normal ($n = 6$) and maximally vasodilated hearts ($n = 6$). The grey lines denote the mean mitoPO$_2$.

Table 2
Functional characteristics of isolated Langendorff-perfused rat hearts

O_2 % perfusate	Flow ml/min/G_{ww}	P_{perf} mm Hg	P_{sys} mm Hg	P_{dia} mm Hg	VPO_2 mm Hg	MVO_2mol/min/G_{ww} µmol/min/G_{ww}	RPP($\times 10^3$) mm Hg/min
95	13.3 ± 0.8	78 ± 2	117 ± 7	2 ± 1	153 ± 9	9.3 ± 0.5	35.1 ± 2.2
70	13.3 ± 0.8	80 ± 5	105 ± 12	2 ± 1	82 ± 7	7.4 ± 0.4	31.6 ± 3.5
45	13.3 ± 0.8	89 ± 11	71 ± 7	2 ± 1	36 ± 4	5.1 ± 0.2	21.4 ± 2.2
95	23.1 ± 0.7	79 ± 1	138 ± 5	2 ± 1	295 ± 21	11.8 ± 0.8	41.4 ± 1.5
70	23.1 ± 0.7	83 ± 4	123 ± 7	2 ± 1	205 ± 14	9.1 ± 0.6	35.1 ± 1.9
45	23.1 ± 0.7	96 ± 7	106 ± 8	2 ± 1	91 ± 11	7.1 ± 0.5	31.7 ± 2.1

Values are given for hearts ($n = 6$) perfused at normal vasodilatation (normal flow) and at maximal vasodilatation ($n = 6$; high flow) for different % oxygen in the perfusate. G_{ww} = gram, wet weight; P_{perf} = perfusion pressure; P_{sys} = systolic pressure; P_{dia} = diastolic pressure; VPO_2 = venous oxygen tension; MVO_2 = oxygen consumption, RPP = rate pressure product (P_{sys} × heart rate). Values are given as mean ± SEM.

In separate experiments, we measured microvascular PO_2 (μPO_2) using the exogenous dye Pd-porphyrin for the three different FiO_2. μPO_2 amounted to 67 ± 3, 108 ± 9 and 22 ± 4 mm Hg, at 40%, 100% and 10% FiO_2, respectively.

3.7. MitoPO_2 in the Langendorff-perfused heart

Delayed fluorescence signals were obtained from isolated hearts, showing decreasing decay times (shorter τ) with increasing percentage of oxygen (%O_2) in the perfusate or with increased flow (going from the normal vasodilated to the maximal vasodilated condition) (Fig. 5A). The recovery of mitoPO_2 histograms provides a detailed view of the effects of %O_2 and vasodilatation on mitochondrial oxygenation (Fig. 5B). Only at maximal oxygenation (95%) and maximal vasodilatation did mitoPO_2 start to approach a normal distribution in the isolated heart, with a mean mitoPO_2 of 40 ± 3 mm Hg. The normally perfused Langendorff-condition had a mean mitoPO_2 of 29 ± 5 mm Hg (at 95% oxygen). A dichotomous distribution was observed, with the largest fraction of mitochondria falling into the lowest oxygen range (0–10 mm Hg). The fraction of mitochondria in the lowest oxygen range increased further as the % O_2 was decreased to 70% and 45%. Decreasing %O_2 was associated with decreased mechanical performance and oxygen consumption of the hearts, whereas maximal vasodilatation increased mechanical performance and oxygen consumption (Table 2). It should be noted that oxygen consumption increased with vasodilation due to the large coronary flow increases, despite the increase in venous PO_2 with vasodilation for each level of %O_2 perfusate. Increasing the heart rate from 300 to 400 BPM did not change the mitoPO_2 distribution in hearts without vasodilation (Fig. 6). In hearts with maximal vasodilation there appeared to be a tendency towards lower mitoPO_2 values at higher heart rate without reaching significance in any of the bins (paired non-parametric testing).

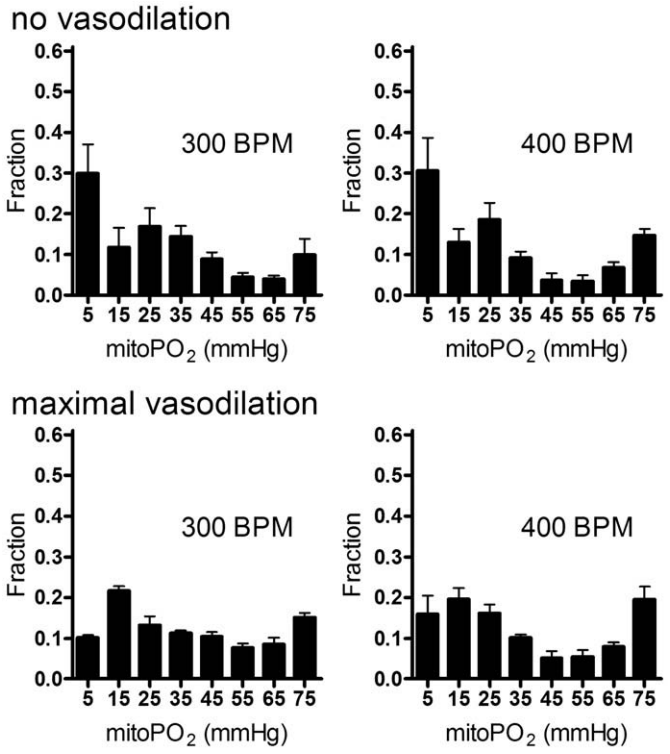

Fig. 6. Response of mitoPO_2 to a heart rate step in the Langendorff-perfused heart. Distributions of mitoPO_2 at 300 and 400 beats per minute (BPM) with and without maximal vasodilation and with 95% oxygen saturated perfusate.

4. Discussion

This study is, to our knowledge, the first to describe direct measurements of mitochondrial oxygen tension within the intact heart. The main findings provide evidence that mean cardiac mitoPO_2 in vivo has a relatively high value of 35 mm Hg. Importantly, we found that mitoPO_2 was heterogeneously distributed within the rat heart in vivo, such that even when mean mitoPO_2 was 35 mm Hg, 10% of mitochondria still had a low PO_2 between 0 and 10 mm Hg. In addition, the frequently used isolated heart preparation operates at a lower mitochondrial oxygenation status than that of the in vivo heart.

4.1. In vivo myocardial PO_2 and mitoPO_2 heterogeneity

Because oxygen transport to the mitochondria is driven by a concentration gradient determined by consumption in the mitochondria, the oxygen tension in the mitochondrial compartment should be at the lowest end of oxygen tensions present compared to other [4] compartments (vascular, interstitial, cytosolic) of the intact heart. The mean mitoPO_2 value of 35 ± 5 mm Hg reported here is in accordance with tissue PO_2 values of 45 ± 8 mm Hg [13] and microvascular PO_2 values of 50–70 mm Hg found in the present and past studies [12], but is much higher than anticipated from estimates derived from cytosolic/interstitial/vascular measurements of 3–17 mm Hg [6–11]. Interestingly, this observation coincides with recent findings of oxygen pressure in tissues other than heart [30]. Myoglobin saturation studies in in vivo pig hearts, using either optical reflectance spectroscopy [31] or ^{1}H NMR [32], were unable to detect desaturation of myoglobin. Knowing that these techniques can detect myoglobin desaturation only when intracellular PO_2 falls below 22 mm Hg [32], and that only an average myoglobin saturation is detected, these studies indicate an average cytosolic PO_2 above 22 mm Hg. Thus, the values obtained with myoglobin saturation techniques are commensurate with our averaged mitoPO_2 of 35 mm Hg. Only recently has consensus been reached that the levels of oxygen in the tissue are much higher than originally thought of, due to the development of new techniques with increased accuracy [30]. The present study with the use of a novel technique clearly indicates that this new consensus may also hold for the heart.

Although the averaged mitoPO$_2$ observed in vivo was higher than anticipated, it is important to take into account the heterogeneity of mitoPO$_2$ within the heart. The observed heterogeneity in mitoPO$_2$ in the present study extends previously observed heterogeneities in, for example, blood flow and oxygen consumption down to the level of the mitochondria [12,16,17]. In addition, the mitoPO$_2$ heterogeneity indicates that approximately 10% of the mitochondria in the in vivo heart are exposed to a PO$_2$ between 0 and 10 mm Hg. Isolated mitochondria studies have demonstrated that mitochondrial oxidative phosphorylation is dependent on oxygen concentrations at PO$_2$<12–15 mm Hg [1,3,5]. This implies that some fraction of the mitochondria within the in vivo heart may well be partially controlled by the prevailing oxygen tension. That myocardial oxygen may be limiting is also supported by studies in myoglobin-knockout mice. Although the first studies in these mice concluded that myoglobin is of no physiological consequence for cardiac function [33], subsequent studies demonstrated that multiple compensatory mechanism in these mice were present [34], indicating an important role for myoglobin in oxygen delivery. Considering the major role that mitochondria play in cellular oxygen sensing [4], the quantitative determination of mitoPO$_2$ in the in vivo condition provides important information for the design of oxygen critical experiments.

4.2. Isolated versus in vivo hearts

In non-vasodilated Langendorff-perfused isolated hearts, the fraction of mitochondria with oxygen tensions between 0 and 10 mm Hg increased to 30%, as compared to the 10% observed in the in vivo condition. Interestingly, studies using three-dimensional microvascular modeling together with myoglobin saturation information [35,36] have also concluded that approximately 15–30% of the myocardium in the Langendorff-perfused heart was hypoxic. Alleviating the 30% "hypoxic mitochondrial area" to 10% by increasing perfusate flow was indeed accompanied by increased myocardial oxygen consumption and mechanical performance, suggesting at least that the normal perfused isolated heart was oxygen limited. This data agree with older literature suggesting that the isolated heart is partially hypoxic [37,38]. Our data indicate that the oxygenation status of the isolated Langendorff-perfused heart model is comparable to that of the in vivo heart only in the maximally vasodilated condition.

4.3. Methodological considerations

The PpIX delayed fluorescence technique provides a powerful tool for monitoring mitoPO$_2$ in cardiac muscle. The underlying lifetime technology is highly robust in that it needs no recalibration and is immune to changes in tissue optical properties and tissue geometry, important features in a beating heart. A practical advantage is also that the technique does not need a physical contact with the heart, like oxygen electrodes, and is not locally destructive. As an optical technique it is scalable from microscopic to macroscopic implementations providing extensive opportunities for study of the heterogeneity of mitoPO$_2$ and its cause. Because of its resemblance to phosphorescence lifetime measurements further technological developments could provide e.g. imaging [39], 3-dimensional scanning by two-photon excitation [40] and multi-wavelength excitation [29]. The main disadvantage is the relatively small penetration depth of light in tissues. Therefore the technique is not non-invasive for the whole organism (like e.g. MRI), but one always needs to make the organ or tissue accessible to the optical device.

In the present study we converted lifetime distribution to oxygen histograms, based on the assumption that the heterogeneity in delayed fluorescence lifetimes arises from a volume with homogeneous distribution of PpIX and heterogeneous concentration of oxygen [19]. Such an assumption is generally relied on when converting phosphorescence lifetime distributions into quencher distributions [19,41,42]. In the present study, fluorescence microscopy of freshly isolated cardiomyocytes from ALA-treated animals showed the typical mitochondrial fluorescence patterns well known from NADH autofluorescence microscopy [43,44], indicating that PpIX synthesis is not sequestered within a cardiomyocyte. On a more macroscopic level, ALA administration induces a diffuse and near homogenous PpIX fluorescence throughout the heart as observed by the cryomicrotome and flow cytometry experiments.

Based on the work of Gandjbakhche et al. [45] the measurement depth with excitation at 510 nm is estimated to be between 400 and 500 μm, due to absorption and scatter of the excitation light. Sinaasappel et al. [46] estimated a catchment depth of 500 μm, using Monte-Carlo simulations on the penetration depth of 520 nm excitation light in phosphorescence lifetime measurements in the intestine. Assuming a left ventricular free wall thickness of 1.5 mm during diastole and 2.5–3.0 mm during systole, our mitoPO$_2$ measurements mainly reflect the oxygenation of the epicardium. Therefore, the mitoPO$_2$ distributions are unlikely to be caused by differences in endocardial and epicardial oxygenation. We previously demonstrated in rat liver that diffusion of ambient oxygen into the tissue has limited influence on the shape of mitoPO$_2$ histograms [14]. Oxygen in the ambient atmosphere marginally contributes to the highest PO$_2$ bins without altering the overall shape of the histograms. Exposure of epicardial surface to air is therefore very likely not the cause of the observed heterogeneity in mitoPO$_2$.

The delayed fluorescence lifetime in vivo may also be affected by bound versus unbound PpIX and pH. Theoretically, unbound PpIX could mimic a very high PO$_2$ and distort the mitoPO$_2$ histograms. Unbound PpIX has a lifetime which is too short to be resolved with our current setup and therefore will not contribute to our signal. Furthermore, binding of PpIX with different environments could affect the lifetime measurements by introducing additional lifetimes at a homogenous PO$_2$. However, the linear relationship between reciprocal delayed fluorescence lifetime and PO$_2$ after abolishing oxygen gradients by addition of cyanide, as predicted by the Stern–Volmer equation [26,47] and obtained by monoexponential fitting on the data, argues against such influence. Physiological changes in pH have in general only minor effects on the quenching constants of phosphorescence [26,48,49] and delayed fluorescence [15]. Overall, despite the assumptions made in the current analysis and the possible caveats this introduces into the interpretation of the data, we regard PpIX delayed fluorescence as a valuable addition to the arsenal of techniques that allows new insight into myocardial oxygenation.

In summary, the data of the present study revealed that the amount of oxygen present within the mitochondria of the intact heart is higher than previously anticipated, is heterogeneously distributed and is lower in the often-used tyrode perfused isolated heart model as compared to the in vivo heart. Together, these results provide a first quantitative characterization of mitochondrial oxygenation within the intact heart in both the in vivo and isolated condition.

Acknowledgments

This work was partly sponsored by The Netherlands Organization for Scientific Research (ZON-MW 911-05-008) and in part by a Technological Collaboration Grant (TSGE 1048) from the Dutch Ministry of Economic Affairs. J. Stap was funded in part by a grant from the Dutch Cancer Society.

References

[1] Hoffman DL, Salter JD, Brookes PS. Response of mitochondrial reactive oxygen species generation to steady-state oxygen tension: implications for hypoxic cell signaling. Am J Physiol, Heart Circ Physiol 2007;292:H101–8.
[2] Maxwell PH, Wiesener MS, Chang GW, Clifford SC, Vaux EC, Cockman ME, et al. The tumour suppressor protein VHL targets hypoxia-inducible factors for oxygen-dependent proteolysis. Nature 1999;399:271–5.

[3] Rumsey WL, Schlosser C, Nuutinen EM, Robiolio M, Wilson DF. Cellular energetics and the oxygen dependence of respiration in cardiac myocytes isolated from adult rat. J Biol Chem 1990;265:15392–402.
[4] Ward JP. Oxygen sensors in context. Biochim Biophys Acta 2008;1777:1–14.
[5] Wilson DF, Rumsey WL, Green TJ, Vanderkooi JM. The oxygen dependence of mitochondrial oxidative phosphorylation measured by a new optical method for measuring oxygen concentration. J Biol Chem 1988;263:2712–8.
[6] Rumsey WL, Pawlowski M, Lejavardi N, Wilson DF. Oxygen pressure distribution in the heart in vivo and evaluation of the ischemic "border zone". Am J Physiol 1994;266:H1676–80.
[7] Trochu JN, Bouhour JB, Kaley G, Hintze TH. Role of endothelium-derived nitric oxide in the regulation of cardiac oxygen metabolism: implications in health and disease. Circ Res 2000;87:1108–17.
[8] Zhao X, He G, Chen YR, Pandian RP, Kuppusamy P, Zweier JL. Endothelium-derived nitric oxide regulates postischemic myocardial oxygenation and oxygen consumption by modulation of mitochondrial electron transport. Circulation 2005;111:2966–72.
[9] Gayeski TE, Honig CR. Intracellular PO_2 in individual cardiac myocytes in dogs, cats, rabbits, ferrets, and rats. Am J Physiol 1991;260:H522–31.
[10] Gnaiger E, Lassnig B, Kuznetsov A, Rieger G, Margreiter R. Mitochondrial oxygen affinity, respiratory flux control and excess capacity of cytochrome *c* oxidase. J Exp Biol 1998;201:1129–39.
[11] Wittenberg BA, Wittenberg JB. Transport of oxygen in muscle. Annu Rev Physiol 1989;51:857–78.
[12] Zuurbier CJ, van Iterson M, Ince C. Functional heterogeneity of oxygen supply–consumption ratio in the heart. Cardiovasc Res 1999;44:488–97.
[13] Al-Obaidi MK, Etherington PJ, Barron DJ, Winlove CP, Pepper JR. Myocardial tissue oxygen supply and utilization during coronary artery bypass surgery: evidence of microvascular no-reflow. Clin Sci (Lond) 2000;98:321–8.
[14] Mik EG, Johannes T, Zuurbier CJ, Heinen A, Houben-Weerts JH, Balestra GM, et al. In vivo mitochondrial oxygen tension measured by a delayed fluorescence lifetime technique. Biophys J 2008;95:3977–90.
[15] Mik EG, Stap J, Sinaasappel M, Beek JF, Aten JA, van Leeuwen TG, et al. Mitochondrial PO_2 measured by delayed fluorescence of endogenous protoporphyrin IX. Nat Methods 2006;3:939–45.
[16] Decking UK. Spatial heterogeneity in the heart: recent insights and open questions. News Physiol Sci 2002;17:246–50.
[17] Yipintsoi T, Dobbs Jr WA, Scanlon PD, Knopp TJ, Bassingthwaighte JB. Regional distribution of diffusible tracers and carbonized microspheres in the left ventricle of isolated dog hearts. Circ Res 1973;33:573–87.
[18] Takahashi E. Anoxic cell core can promote necrotic cell death in cardiomyocytes at physiological extracellular PO_2. Am J Physiol, Heart Circ Physiol 2008;294: H2507–15.
[19] Golub AS, Popel AS, Zheng L, Pittman RN. Analysis of phosphorescence in heterogeneous systems using distributions of quencher concentration. Biophys J 1997;73:452–65.
[20] Kammermeier H. Isolated, (Langendorff) hearts perfused with an aqueous buffer (should) have excess oxygen availability. Basic Res Cardiol 1994;89:545–8.
[21] ter Welle HF, Baartscheer A, Fiolet JW, Schumacher CA. The cytoplasmic free energy of ATP hydrolysis in isolated rod-shaped rat ventricular myocytes. J Mol Cell Cardiol 1988;20:435–41.
[22] Spaan JA, ter Wee R, van Teeffelen JW, Streekstra G, Siebes M, Kolyva C, et al. Visualisation of intramural coronary vasculature by an imaging cryomicrotome suggests compartmentalisation of myocardial perfusion areas. Med Biol Eng Comput 2005;43:431–5.
[23] Heinen A, Camara AK, Aldakkak M, Rhodes SS, Riess ML, Stowe DF. Mitochondrial Ca2+-induced K+ influx increases respiration and enhances ROS production while maintaining membrane potential. Am J Physiol, Cell Physiol 2007;292:C148–56.
[24] Heinen A, Huhn R, Smeele KM, Zuurbier CJ, Schlack W, Preckel B, et al. Helium-induced preconditioning in young and old rat heart: impact of mitochondrial Ca (2+)-sensitive potassium channel activation. Anesthesiology 2008;109:830–6.
[25] Nunn JF, Bergmann NA, Coleman AJ. Factors influencing the arterial oxygen tension during anaesthesia with artificial ventilation. 1965. Br J Anaesth 1998;80:860–76.
[26] Sinaasappel M, Ince C. Calibration of Pd-porphyrin phosphorescence for oxygen concentration measurements in vivo. J Appl Physiol 1996;81:2297–303.
[27] Mik EG, Donkersloot C, Raat NJ, Ince C. Excitation pulse deconvolution in luminescence lifetime analysis for oxygen measurements in vivo. Photochem Photobiol 2002;76:12–21.
[28] Zuurbier CJ, Ince C. Post-ischaemic changes in the response time of oxygen consumption to demand in the isolated rat heart are mediated partly by calcium and glycolysis. Pflugers Arch 2002;443:908–16.
[29] Johannes T, Mik EG, Ince C. Dual-wavelength phosphorimetry for determination of cortical and subcortical microvascular oxygenation in rat kidney. J Appl Physiol 2006;100(4):1301–10.
[30] Wilson DF. Quantifying the role of oxygen pressure in tissue function. Am J Physiol, Heart Circ Physiol 2008;294:H11–3.
[31] Arai AE, Kasserra CE, Territo PR, Gandjbakhche AH, Balaban RS. Myocardial oxygenation in vivo: optical spectroscopy of cytoplasmic myoglobin and mitochondrial cytochromes. Am J Physiol 1999;277:H683–97.
[32] Murakami Y, Zhang Y, Cho YK, Mansoor AM, Chung JK, Chu C, et al. Myocardial oxygenation during high work states in hearts with postinfarction remodeling. Circulation 1999;99:942–8.
[33] Garry DJ, Ordway GA, Lorenz JN, Radford NB, Chin ER, Grange RW, et al. Mice without myoglobin. Nature 1998;395:905–8.
[34] Godecke A, Flogel U, Zanger K, Ding Z, Hirchenhain J, Decking UK, et al. Disruption of myoglobin in mice induces multiple compensatory mechanisms. Proc Natl Acad Sci U S A 1999;96:10495–500.
[35] Beard DA, Schenkman KA, Feigl EO. Myocardial oxygenation in isolated hearts predicted by an anatomically realistic microvascular transport model. Am J Physiol, Heart Circ Physiol 2003;285:H1826–36.
[36] Ejike JC, Arakaki LS, Beard DA, Ciesielski WA, Feigl EO, Schenkman KA. Myocardial oxygenation and adenosine release in isolated guinea pig hearts during changes in contractility. Am J Physiol, Heart Circ Physiol 2005;288:H2062–7.
[37] Heineman FW, Kupriyanov VV, Marshall R, Fralix TA, Balaban RS. Myocardial oxygenation in the isolated working rabbit heart as a function of work. Am J Physiol 1992;262:H255–67.
[38] van Beek JH, Bouma P, Westerhof N. Oxygen uptake in saline-perfused rabbit heart is decreased to a similar extent during reductions in flow and in arterial oxygen concentration. Pflugers Arch 1989;414:82–8.
[39] Rumsey WL, Vanderkooi JM, Wilson DF. Imaging of phosphorescence: a novel method for measuring oxygen distribution in perfused tissue. Science 1988;241: 1649–51.
[40] Mik EG, van Leeuwen TG, Raat NJ, Ince C. Quantitative determination of localized tissue oxygen concentration in vivo by two-photon excitation phosphorescence lifetime measurements. J Appl Physiol 2004;97:1962–9.
[41] Vinogradov SA, Fernandez-Seara MA, Dupan BW, Wilson DF. A method for measuring oxygen distributions in tissue using frequency domain phosphorometry. Comp Biochem Physiol A Mol Integr Physiol 2002;132:147–52.
[42] Vinogradov SA, Wilson DF. Phosphorescence lifetime analysis with a quadratic programming algorithm for determining quencher distributions in heterogeneous systems. Biophys J 1994;67:2048–59.
[43] Eng J, Lynch RM, Balaban RS. Nicotinamide adenine dinucleotide fluorescence spectroscopy and imaging of isolated cardiac myocytes. Biophys J 1989;55:621–30.
[44] Takahashi E, Endoh H, Doi K. Intracellular gradients of O_2 supply to mitochondria in actively respiring single cardiomyocyte of rats. Am J Physiol 1999;276: H718–24.
[45] Gandjbakhche AH, Bonner RF, Arai AE, Balaban RS. Visible-light photon migration through myocardium in vivo. Am J Physiol 1999;277:H698–704.
[46] Sinaasappel M, van Iterson M, Ince C. Microvascular oxygen pressure in the pig intestine during haemorrhagic shock and resuscitation. J Physiol 1999;514: 245–53.
[47] Vanderkooi JM, Berger JW. Excited triplet states used to study biological macromolecules at room temperature. Biochim Biophys Acta 1989;976:1–27.
[48] Dunphy I, Vinogradov SA, Wilson DF. Oxyphor R2 and G2: phosphors for measuring oxygen by oxygen-dependent quenching of phosphorescence. Anal Biochem 2002;310:191–8.
[49] Lo LW, Koch CJ, Wilson DF. Calibration of oxygen-dependent quenching of the phosphorescence of Pd-meso-tetra (4-carboxyphenyl) porphine: a phosphor with general application for measuring oxygen concentration in biological systems. Anal Biochem 1996;236:153–60.